VIS-NIR SPECTRAL CONTINUUM SLOPE OF LUNAR HIGH LATITUDE REGIONS OBSERVED BY SELENE SPECTRAL PROFILER. Y. Yokota[1], T. Matsunaga[1], M. Ohtake[2], J. Haruyama[2], R. Nakamura[3], S. Yamamoto[1], S. Sasaki[4], T. Hiroi[5], Y. Ogawa[6], C. Honda[6], T. Morota[7], and Y. Ishihara[3], [1]National Institute for Environmental Studies, 16-2 Onogawa, Tsukuba, Ibaraki 305-8506, Japan (yokota.yasuhiro@nies.go.jp), [2]ISAS, JAXA, Japan, [3]National Institute of Advanced Industrial Science and Technology, Japan, [4]National Astronomical Observatory of Japan, [5]Brown Univ., [6] Univ. Aizu, Japan, and [7]Nagoya Univ., Japan.

Introduction: Based on the Vis-NIR observation data from the lunar explorer SELENE (Kaguya), it was reported that the lunar high latitude (>~75°) regions in both the north and south have much lower spectral continuum slopes than the low and medium latitude regions [1]. At the high latitude regions, the spectral continuum slope which is measured by the ratio of radiance factor between 1548 nm band and 753 nm band (hereafter color ratio r_{1548}/r_{753}) is lower than ~1.8. This low color ratio implies low degrees of space weathering. In the previous studies of space weathering (e.g., [2, 3]), it is considered that protons in the solar wind have a role to reducing Fe from the silicate at the lunar surface. Therefore, this color anomaly perhaps indicates local shortage of the protons for the space weathering process.

This hypothesis leads to a new question. At the high latitude region, a surface facet which inclined toward the equator may be able to collect more protons than a horizontal facet. Is there a difference of the color ratio between the inclined facet and horizontal facet?

In this study, we conduct a detailed analysis for the distribution of the low spectral continuum slope area in the lunar high latitude regions.

Data and method:

Topography data. The gridded topography map by SELENE Laser altimeter (LALT) [4] data product (LALT_GGT_MAP) is used to compute the inclination of the lunar surface. This map has 1/16 degree (~1.9 km in North-South direction) spatial resolution. This product was publicly released through the SELENE Data Archive (http://l2db.selene.darts.isas.jaxa.jp/index.html.en).

Indicator of surface inclination. We define an angle θ as shown in Figure 1. For the convinience of computation, only North-South directional topography profile is used. N is a normal vector of the lunar surface in the North-South cross section plane. E is a vector parallel to the equitorial plane. We employ the cos θ value as an indicator for the efficiency to collect the solar wind protons.

Polar stereographic maps of cos θ are made from the LALT gridded topography map. The mesh size of the output maps are ~3.4 km at the center (pole). The average cos θ is stored for each mesh.

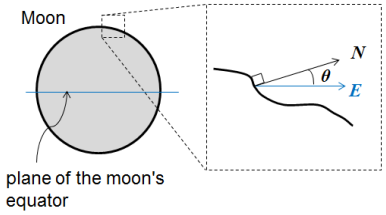

Figure 1. Definition of θ.

Reflectance spectral data. The SELENE Spectral Profiler (SP) measured lunar Vis–NIR spectral reflectance in an instantaneous field of view of ~550 m from a 100-km-altitude orbit [5]. We used nearly 7000 orbits of radiometrically [6] and photometrically corrected SP data (SP L2C product). One orbit contains over 10,000 spectra.

The SP L2C product contains two types of photometrically corrected radiance factor based on the method in [1], namely, the high-albedo group correction and the low albedo group correction. Since the high latitude regions are mainly highlands, we use the high-albedo group correction data.

The viewing geometry in the photometric correction were calculated for a spherical lunar model. If we take into account the undulation of lunar surface topography, the incidence angle i and emission angle e will be changed. On the other hand, the phase angle α is not changed by topography. Based on the following assumption, we do not use absolute value of the radiance factor in the analysis. (1) The phase angle mainly controls photomitric color change of lunar surface, and this effect is already corrected in SP L2C product by the present correction method. (2) Although the variation of i and e affect the brightness for all bands, such effect is canceled out in the color ratio.

Several methods are proposed by previous studies [e.g. 7, 8] to indicate optical maturity from Vis-NIR reflectance spectra. those methods require the absolute value of the reflectance. However, the absolute value cannot used in this study due to the above mentioned situation. Therefore, we simply employ the color ratio r_{1548}/r_{753} as the indicator of the steepness of the continuum slope. We should notice that such simple indicator is also affected by mineral composition. For example,

Mare generally have a higher color ratio r_{1548}/r_{753} than highlands [1].

Color ratio map. We make polar stereographic maps of the color ratio by a procedure similar to that of the 1° mesh map in [1]. Data for $\alpha > 85°$ were excluded because of the low solar elevation limitation of the photometric correction.

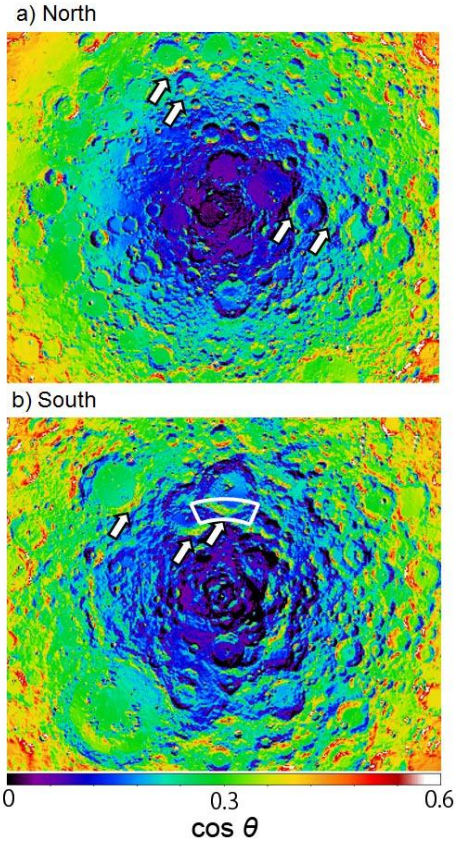

Figure 2. Maps of cos θ.

Results: Figure 2a and b are the maps of cos θ value for the north-pole and south-pole, respectively. Figure 3c and d depict the maps for the color ratio r_{1548}/r_{753} with higher spatial resolution than [1].

It is revealed that the color ratio roughly correlates with the cos θ value at many points in Figure 2 and 3. Seven easily-noticeable points of them are indicated by arrows in the figure for example.

Figure 4 depict the cos θ vs. color ratio plot example for the the white arc region indicated in Figure 2b (S81–S83°, E250–290°). The low cos θ data (<0.1) are excluded because of low S/N. The plot show moderate correlation (R=0.57). This may support the hypothesis that the inclination of the facets affect the optical maturity at the high latitude regions.

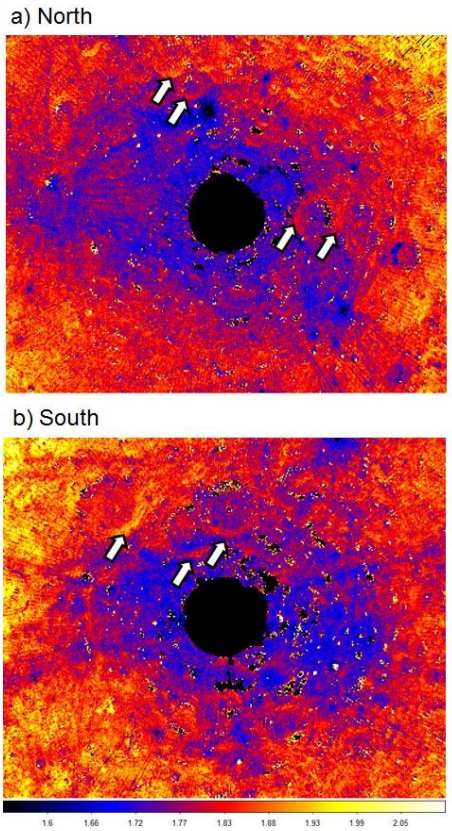

Figure 3. Maps of color ratio r_{1548}/r_{753}. The color bar range is 1.5 to 2.1.

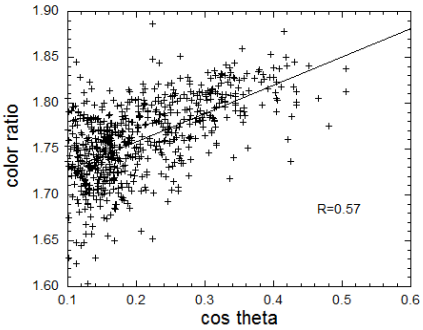

Figure 4. The cos θ vs. color ratio r_{1548}/r_{753} plot for the white arc region in Figure 2b.

References: [1] Yokota Y. et al. (2011) *Icarus*, *215*, 639–660. [2] Housley R. et al. (1973) *Proc. Lunar Plaent. Sci. Conf. 4th*, 2737–2749. [3] Hapke B. (2001) *JGR*, *106*(E5), 10,039–10,073. [4] Araki H. et al. (2009) *Science 323*, 897. [5] Matsunaga T. et al. (2008) *GRL*, *35*, L23201. [6] Yamamoto S. et al. (2011) *IEEE Transactions on Geosci. and Remote Sensing*, *49*, 11, 4660-4676. [7] Hiroi T. et al. (1997) *LPS XXVIII*, Abstract 1152. [8] Lucey, P.G. et al. (2000) *JGR 105 (E8)*, 20297–20305.